# Synthesis and Optical Characterization of Au/Ag Core/Shell Nanorods

**Mingzhao Liu and Philippe Guyot-Sionnest***

*James Frank Institute, The University of Chicago, 5640 South Ellis Avenue, Chicago, Illinois 60637*

*Received: November 28, 2003; In Final Form: February 23, 2004*

Au/Ag core/shell nanorods with different shell thickness were synthesized in aqueous solution by chemically depositing silver on gold nanorods surface. With the silver coating, the longitudinal plasmon mode of the nanorods shifted blue and was enhanced. A dipole-limit calculation, based on confocal ellipsoids, simulates the spectra of the core/shell nanorods using bulk dielectric functions. Good agreement with the experimental result was achieved. Light scattering spectra of single nanorods were taken by dark-field microscopy to measure the homogeneous line width. The scattering spectra of single gold nanorods are less than 10% broader than the theoretical value, while the spectra of silver-coated nanorods are systematically 40−50% broader. The additional damping of the plasmon was modeled as the extra scattering at the Au−Ag interface and the nanorods surface. A model for evaluating the plasmon damping in inhomogeneous metallic systems with interfaces is presented.

## 1. Introduction

Since the discovery of SERS (surface-enhanced Raman spectroscopy),[1,2] there has been a growing interest in studying the near-field properties of metal colloids. The induced oscillation of free electrons in the metal nanoparticles, known as surface plasmon,[3] drastically disturb the near-field at the resonance and give strong light scattering and absorption, in addition to huge local field enhancement.[4] One of the features of the plasmon resonance is its strong shape dependence.[5,6] For example, the single plasmon resonance mode in a noble metal nanosphere is split into two modes as the sphere is distorted into prolate spheroid (or rod), with one blue-shifted (transverse) and another red-shifted (longitudinal).[6,7] Simply by varying the shape or composition of the metal nanoparticles, strongly colored solutions can be obtained that cover a wide spectral range (Figure 1).

As shown by both calculation and experiment, the rod-shaped metal nanoparticles show a much greater local field enhancement and therefore a more significant SERS activity than metal nanospheres.[8,9] During the past decades, different template-based methods have been developed to prepare metal nanorods that can be dispersed in liquid. Van der Zande et al. used porous alumina as a hard template for electrodeposition of gold into nanorods with various aspect ratios, and obtained aqueous dispersions of nanorods by dissolving the alumina template.[10] Soft template methods were also developed. Gold nanorods were synthesized using a cationic surfactant, CTAB (cetyltrimethylammonium bromide),[11−14] which was shown to form rodlike micelles in aqueous solution.[15] Murphy et al. developed the seed-mediated growth technique for preparing gold nanorods, which can be processed under a large scale.[12] Compared to the hard-template method, the surfactant-based method usually gives a more regular shape and therefore better spectral property. By varying the growth conditions, including the amount and size of seed particles, pH of the solution, and concentration of surfactants, gold nanorods with aspect ratio 2−20 can be synthesized.[12,14] Correspondingly, the longitudinal plasmon mode is tuned from the visible region to the near-infrared (Figure 2).

Silver is used most commonly in the SERS study,[17] because its *d*−*s* band gap is in the UV region and does not damp out the plasmon mode as strongly as for gold.[18] However, monodispersed silver nanorods have not yet been characterized. As a possible replacement of pure silver nanorods, Jang et al. deposited silver onto gold nanorods and measured their SP absorption spectra.[19] In this paper, we present a different but simpler approach and we carry out the modeling of the extinction spectra.

Another interesting topic arises from plasmon damping by interfaces, both the silver−gold interface and the medium−silver interface. To evaluate the extra damping associated with the Au/Ag interface and the thin silver coating, we measured the optical scattering spectra of single nanorods. We present a new model to account for the effect of interfacial scattering on the plasmon line width.

## 2. Experimental Section

**A. Preparation of Au/Ag Core/Shell Nanorods.** Ascorbic acid was purchased from Fluka. All the other chemicals used in this experiment were purchased from Sigma-Aldrich without further purification. Gold nanorods with diameter 15 nm and aspect ratio 3 were synthesized via a seed-mediated method developed by El-Sayed et al.[14] The gold nanorods solution was stored for at least 24 h before use. Two different procedures were used to coat the gold nanorods with silver.

*A.1. Colloids Stabilized by Citrate.* A quantity of 0.8 mL of gold nanorods solution ($c_{Au} = 0.5$ mM) was added to 4 mL of 15 wt % sodium citrate solution. To this solution, various amounts (0.1, 0.25, 0.5, 0.8 mL) of 1.0 mM $AgNO_3$ solution were added to the gold nanorods solution with gentle mixing. Finally, 0.5 mL of 5 wt % ascorbic acid was injected into the solution to start the reaction. The reduction went to completion in 5−10 min, during which the color of the solution changed from light gray to green, bluish green, and purplish red, upon increasing the amount of silver.

* Corresponding author. E-mail: pgs@midway.uchicago.edu.

10.1021/jp037644o CCC: $27.50 
Published on Web 04/16/2004

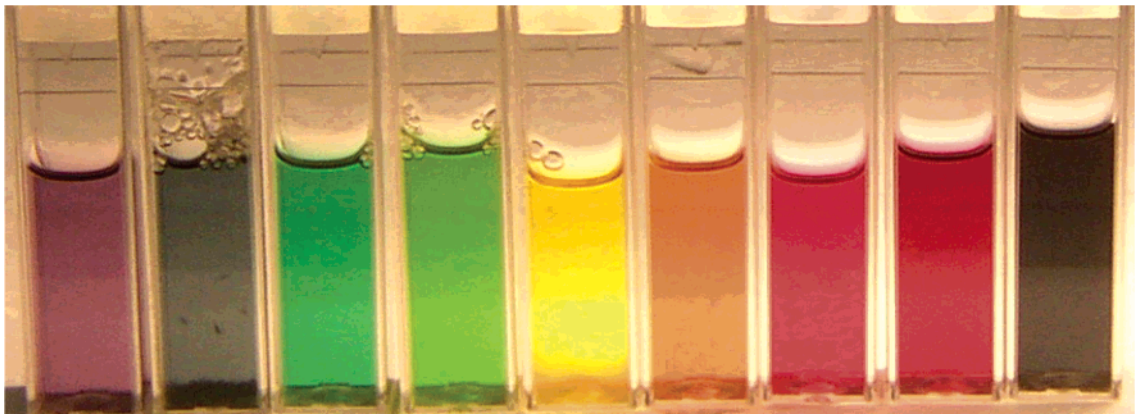

**Figure 1.** Metal colloid solutions of gold and silver nanoparticles of different sizes, composition, and with sphere or rodlike shape. From left to right, solutions 1, 2, 9 are gold nanorods with plasmon resonance located at 670, 700, 780 nm, respectively; solutions 7, 8 are mixtures of gold nanospheres and nanorods; solutions 3, 4, 6 are Au/Ag core/shell nanorods with plasmon resonance located at 620, 600, 580 nm, respectively; solution 5 is silver nanospheres.

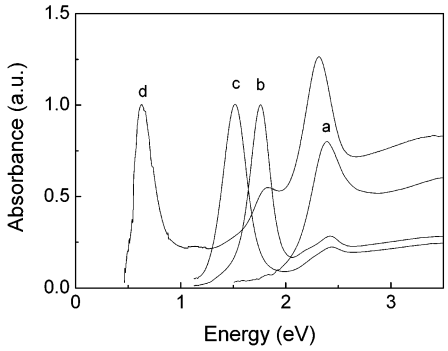


**Figure 2.** Measured absorption spectra of Au nanoparticles. (a) Au nanospheres, $E_{res} = 2.39$ eV. (b) Au nanorods with $R = 3.3$, $E_{res} = 1.76$ eV. (c) Au nanorods with $R = 4.4$, $E_{res} = 1.51$ eV. (d) Au nanorods with $R = 13$, $E_{res} = 0.63$ eV, the significant absorption at 2.31 eV is due to the Au nanospheres as a byproduct. The spectrum of the Au nanorods with $R = 13$ was taken in chloroform solution,[16] while the others were taken in aqueous solutions.

The method proved to be not very reproducible, and the high concentration of sodium citrate caused certain difficulty for taking TEM (transmission electron microscopy) pictures. Considering the disadvantage of this approach, another procedure was used, utilizing a much stronger stabilizing agent.

*A.2. Colloids Stabilized by PVP (polyvinylpyrrolindone).* A quantity of 0.8 mL of gold nanorods solution ($c_{Au} = 0.5$ mM) was diluted into 4 mL of 1 wt % PVP aqueous solution. To this solution, different amount (0.1, 0.25, 0.5, 0.75 mL) of 1.0 mM $AgNO_3$ solution was added, followed by adding 0.1 mL of 0.1 M ascorbic acid and gentle mixing. At this stage, Ag(I) was not reduced due to the low pH of the solution. The reaction was started by injecting 0.2 mL of 0.1 M NaOH solution, followed by quick mixing. The reaction was finished in 1−5 min, with color changes similar to the first procedure.

**B. Measurement.** Gold nanorods and silver-coated nanorods were characterized by TEM to determine the quality of the silver layer and the monodispersity. UV−vis absorption spectra were used to examine how the silver coating affects the surface plasmon resonance of the gold nanorods.

Several approaches for single metal nanoparticles spectroscopy have been developed, including near-field scanning optical[20] and dark-field microscopy.[21−25] In this paper, the light-scattering spectra of single nanorods, either coated with silver or not, were measured by dark-field microscopy, and compared with theoretical calculation. A conventional dark-field microscope setup was used for the measurement of single nanocrystal scattering, with a 100× oil immersion objective, a prism ($n = 1.75$) to give total internal reflection for the dark-field, and a halogen lamp as the light source. The samples were dispersed into ∼3% PVP/methanol solution with the desired concentration, and added dropwise to the surface of the prism. After the evaporation of methanol, a thin PVP film was formed with nanocrystals embedded in it. The scattering from individual metal nanoparticles can be seen by eye with this dark-field microscope setup. For spectral analysis, the scattered light was focused onto the entrance slit of a grating spectrometer, and detected by a nitrogen-cooled CCD camera.

## 3. Results and Discussion

A basic pH is crucial for the reduction of Ag(I) by ascorbic acid.[14] This condition was satisfied automatically in the citrate method (section A.1), since citric acid is a weak acid. In the PVP method (section A.2), it is satisfied by adding 2 M NaOH to neutralize ascorbic acid. CTAB (cetyltrimethylammonium bromide), which was used as the stabilizing agent for gold nanorods, also plays an important role. AgBr has a very low solubility in water but can form small colloids, which may be why the solution remains clear during the reaction. Presumably the formation of AgBr colloid brings the concentration of free $Ag^+$ to a very low level, and therefore Ag(I) can be reduced on the surface of the gold nanorods in a mild way.

The freshly prepared silver-coated gold nanorods solutions show strong colors, varying from green, bluish green, to purplish red, with an increasing thickness of silver coating. Long-term storage at room temperature causes the coated nanorods to decompose and the solution takes on a yellowish color, characteristic of silver nanoparticles. The lifetime at room temperature is about 3 weeks for nanorods stabilized by citrate, and longer than 2 months for those stabilized by PVP.

The TEM images show a different thickness of homogeneous silver layer coated on the surface of gold nanorods for different amounts of silver added (Figure 4). On the basis of the measurement of over 50 rods for each preparation, the gold nanorods have an average diameter 15 nm and aspect ratio 3.05, with a standard deviation 20%. The thickness of the silver coating was also measured from the TEM images, as 1.5 nm for $x_{Ag} = 0.20$, 3.0 nm for $x_{Ag} = 0.38$, 4.0 nm for $x_{Ag} = 0.55$, and 6.0 nm for $x_{Ag} = 0.65$. The difficulty in accurately identifying the Au−Ag interface prevents us from measuring

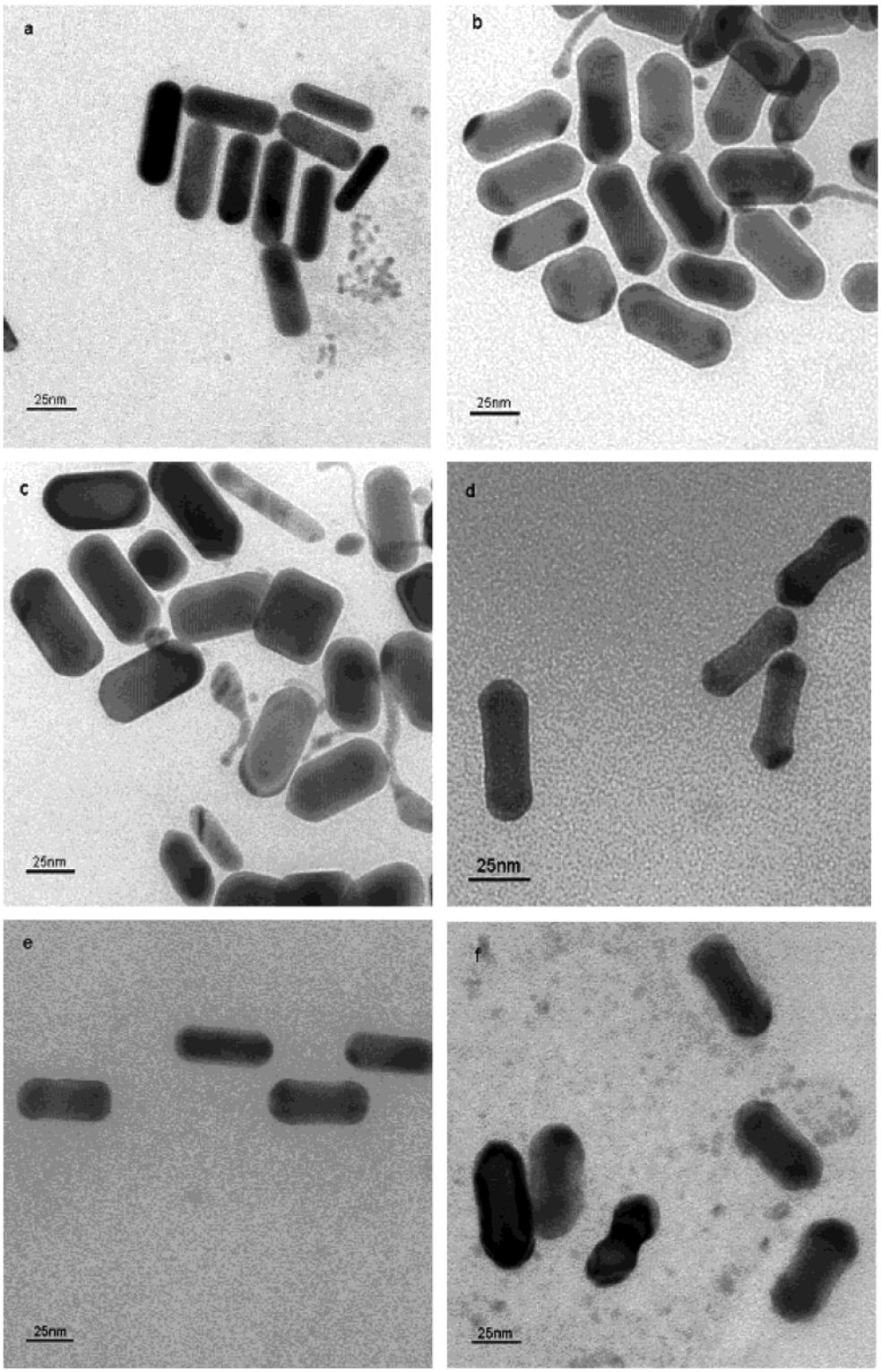


**Figure 3.** TEM images of nanorods. (a) Pure gold nanorods. (b−c) Silver-coated nanorods from the citrate method with $x_{Ag} = 0.38, 0.55$, respectively. (d−f) Silver-coated nanorods from the PVP method with $x_{Ag} = 0.20, 0.38, 0.55$, respectively.

the thickness more quantitatively.[26] Assuming a uniform Ag coating and complete reduction of Ag(I), the expected thicknesses would be 0.75, 1.7, 3.0, and 4.2 nm, respectively.

The visible absorption spectra of freshly prepared gold nanorods and silver-coated gold nanorods are showed in Figure 3. As the silver layer gets thicker, the longitudinal surface plasmon mode blue-shifts. The samples synthesized from the two different procedures have similar spectral properties, indicating that their silver coatings are of similar quality. The blue-shift can arise from two effects. First, the dielectric function of silver is different from gold, therefore the effective dielectric function varies for different thicknesses of silver coating, and second, a homogeneous layer coating of a rod lowers the overall aspect ratio.

As shown by theoretical calculation and experiment, core−shell Au/Ag nanospheres show a completely different spectrum than the alloy particles.[3,26] Therefore, instead of using some "averaged" dielectric function, a simulation on the core−shell structure is needed for further understanding of their spectra.

*Simulation of Core/Shell Spheroid.* An analytically solvable

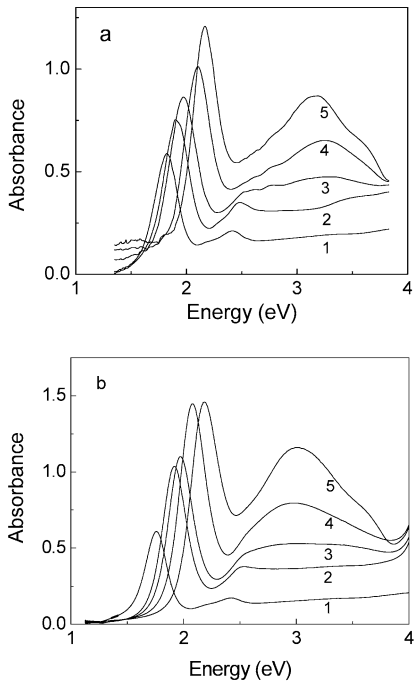


**Figure 4.** (a) Visible spectra of pure gold nanorods (1) and silver-coated gold nanorods prepared by the citrate method (2−5) with molar fraction of silver 20%, 38%, 55%, and 67%, respectively. (b) Visible spectra of pure gold nanorods (1) and silver-coated gold nanorods prepared by the PVP method (2−5) with molar fraction of silver 20%, 38%, 55%, and 65%, respectively. A blue-shift of the longitudinal (low-energy) mode was observed, from 1.8 eV (pure gold) to 2.2 eV (silver-coated).

model of the core/shell rod structure is possible with confocal ellipsoids, where the prolate spheroidal dielectric ($\epsilon_1$) core, with semiaxes $a_1 = b_1 < c_1$, is coated with another confocal spheroidal dielectric ($\epsilon_2$) shell with semiaxes $a_2 = b_2 < c_2$. The confocal condition gives $c_2^2 - a_2^2 = c_1^2 - a_1^2$. The whole rod is immersed in a medium $\epsilon_m$ and oriented randomly. In the dipole approximation, the polarizabilities along the principal axes of the spheroids are[4]

$$\alpha_1 = \alpha_2 = \frac{v\{(\epsilon_2 - \epsilon_m)[\epsilon_2 + (\epsilon_1 - \epsilon_2)(L_1^{(1)} - fL_1^{(2)})] + f\epsilon_2(\epsilon_1 - \epsilon_2)\}}{[\epsilon_2 + (\epsilon_1 - \epsilon_2)(L_1^{(1)} - fL_1^{(2)})][\epsilon_m + (\epsilon_2 - \epsilon_m)L_1^{(2)}] + fL_1^{(2)}\epsilon_2(\epsilon_1 - \epsilon_2)}$$

$$\alpha_3 = \frac{v\{(\epsilon_2 - \epsilon_m)[\epsilon_2 + (\epsilon_1 - \epsilon_2)(L_3^{(1)} - fL_3^{(2)})] + f\epsilon_2(\epsilon_1 - \epsilon_2)\}}{[\epsilon_2 + (\epsilon_1 - \epsilon_2)(L_3^{(1)} - fL_3^{(2)})][\epsilon_m + (\epsilon_2 - \epsilon_m)L_3^{(2)}] + fL_3^{(2)}\epsilon_2(\epsilon_1 - \epsilon_2)} \quad (1)$$

where $v = 4\pi a_2 b_2 c_2/3$ is the volume of the particle, $f = a_1 b_1 c_1/a_2 b_2 c_2$ is the fraction of the total particle volume occupied by the inner spheroid, and $L_1^{(k)}$ and $L_3^{(k)}$ ($k = 1, 2$) are the geometrical factors defined as

$$L_3^{(k)} = \frac{1 - e_k^2}{e_k^2}\left(-1 + \frac{1}{2e_k}\ln\frac{1 + e_k}{1 - e_k}\right) \quad e_k^2 = 1 - \frac{a_k^2}{c_k^2}$$

$$L_1^{(k)} = \frac{1}{2}(1 - L_3^{(k)}) \quad (k = 1,2) \quad (2)$$

Then the absorption and scattering cross sections of a single particle are evaluated by the optical theorem,

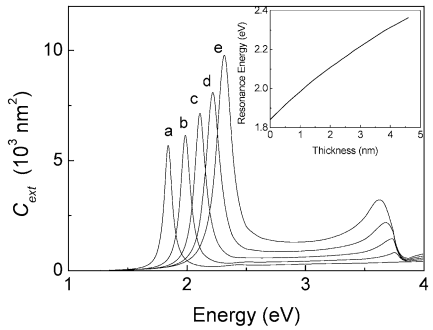


**Figure 5.** Calculated extinction cross sections ($C_{ext} = C_{abs} + C_{sca}$) of randomly oriented nanorods immersed in a medium with $\epsilon_m = 1.77$.[27] The gold core was modeled as a prolate spheroid with a shorter axis 15 nm and aspect ratio 3. The confocally coated silver layers have a thickness at the equator (a) 0 nm (pure gold nanorods), (b) 1 nm, (c) 2 nm, (d) 3 nm, (e) 4 nm. The inset shows a plot of the longitudinal plasmon resonance energy as a function of the thickness of the silver coating.

$$C_{abs} = k\,\mathrm{Im}[(2/3)\alpha_1 + (1/3)\alpha_3]$$

$$C_{sca} = \frac{k^4}{6\pi}[(2/3)|\alpha_1|^2 + (1/3)|\alpha_3|^2] \quad (3)$$

where $k = \omega\epsilon_m^{1/2}/c$ is the wavenumber in the medium.

Figure 4 shows the simulated extinction spectra. They reproduce very well the main feature of the experimental spectra. The strong longitudinal mode shifts from 1.8 eV to 2.3 eV as the silver shell thickness at the equator increases from 0 nm to 4 nm. A weaker transverse mode, which is observed at higher energy, red-shifts slightly and grows as the silver layer gets thicker. This is in qualitative agreement with the experimental spectra in Figure 4. We note, however, that the confocal coating model does not correspond to a uniform coating thickness. Instead, for a prolate spheroid, the coating has the maxima at its equator and the minima at its apex. Therefore as the coating gets thicker, the model reduces the aspect ratio more quickly than the observed uniform coating. As shown in Figure 5, the calculated longitudinal plasmon resonance shifts from 1.8 eV to 2.3 eV, with a 4 nm Ag layer. However, a ~6 nm Ag layer is needed experimentally.

*Homogeneous Width and Model.* It is most notable that the experimental spectra in Figure 4 show a much broader resonance than the simulated ones in Figure 5. Although the inhomogeneous broadening from the size and shape distribution is the main reason, the possible contribution from additional scattering by boundaries should be addressed.[28]

For a noble metal such as gold or silver, the dielectric function can be described as a combination of an interband term $\epsilon_{IB}(\omega)$ and a Drude term:

$$\epsilon_D(\omega) = 1 - \frac{\omega_p^2}{\omega^2 + i\gamma\omega} \quad (4)$$

with the plasma frequency $\omega_p^2 = Ne^2/m\epsilon_0$, where $N$ is the density of free electrons and $m$ is the effective mass of an electron. As the size of the metal particle is comparable to or smaller than $l_\infty$, the mean free path of conduction electron in the bulk, the electron-surface scattering becomes significant.[29] If the scattering is not elastic, an extra size-dependent term is added to the damping $\gamma$. Many models have been developed to evaluate the extra damping due to the finite scattering length imposed by the boundary,[29−31] and most of them resulted in a general phenomenological relation

$$\gamma(L_{\text{eff}}) = \gamma_0 + \frac{A\upsilon_F}{L_{\text{eff}}} \tag{5}$$

where $\gamma_0$ is the bulk damping constant which includes interband contributions. $A$ is a parameter related to the details of the scattering process, $\upsilon_F$ is the Fermi velocity, $L_{\text{eff}}$ is characteristic of the size of the particle, and sometimes referred to as reduced mean free path.

Recently, Coronado and Schatz et al. derived a general geometric expression for $L_{\text{eff}}$ for arbitrary convex nanoparticles, assuming that the electron−surface scattering is totally inelastic. $L_{\text{eff}}$ is then indeed the average chord length between any two points of the surface.[29] For an arbitary convex surface, they obtained the averaged chord length and a very simple expression, $L_{\text{eff}} = 4V/S$, where $V$ and $S$ are the volume and the surface area of the particle, respectively.

The physical meaning of the geometrical mean free path approach is not very obvious. Its main disadvantage is that it is not easily extended to the situation where the electron−surface scattering is partly elastic, and this becomes very restrictive when dealing with a composite system presenting interfaces.

Here we introduce a simpler "integral" approach, by accounting for the energy loss at the surface and in the volume. The method is still a classical phenomenological approach. However, it is intuitively obvious. It is more general since it is not restricted to convex surfaces and it can be applied to any composite systems.

Consider an arbitrary shaped metal particle of volume $V$, surface area $S$, and a surface scattering parameter $0 \le A \le 1$. $A$ is the fraction of electron−surface scattering events that are fully inelastic, the rest being purely elastic. We first treat the simple case of a homogeneous material. The total damping constant can be written as $\gamma = \gamma_0 + \gamma_s$, where $\gamma_0$ is the bulk plasma damping constant, and $\gamma_s$ is the additional damping constant due to the surface. In a time interval d$t$, the number of electrons scattered by the element of surface d$s$ is

$$\mathrm{d}n = \rho\frac{\int_{\mathbf{v}_F\cdot\mathbf{ds}>0}(\mathbf{v}_F\cdot\mathbf{ds})\,\mathrm{d}\Omega}{\int \mathrm{d}\Omega}\mathrm{d}t = \frac{2\pi\rho\int_0^{(\pi/2)}\upsilon_F\cos\theta\sin\theta\,\mathrm{d}\theta}{4\pi}\mathrm{ds}\,\mathrm{d}t = \frac{\rho\upsilon_F}{4}\mathrm{ds}\,\mathrm{d}t \tag{6}$$

where $\rho$ is the density of conduction electrons. The energy loss at the surface $S$ in d$t$ is

$$\mathrm{d}U_s = Au\oint_S \mathrm{d}n = A\frac{u\rho\upsilon_F S}{4}\,\mathrm{d}t = A\frac{\upsilon_F S}{4V}U\,\mathrm{d}t \tag{7}$$

where $u$ is the polarization energy carried by each electron, and $U = u\rho V$ is the total polarization energy. Here we make an assumption that the average polarization energy carried by the surface electrons is equal to $u$, which is satisfied when the particle is homogeneously polarized. Therefore the energy dissipation rate due to the surface inelastic scattering is

$$\gamma_s = A\frac{\upsilon_F S}{4V} \tag{8}$$

Finally, with this short derivation we obtain

$$\gamma = \gamma_0 + \gamma_s = \gamma_0 + A\frac{\upsilon_F S}{4V} \tag{9}$$

which is identical to the result given by Coronado and Schatz.

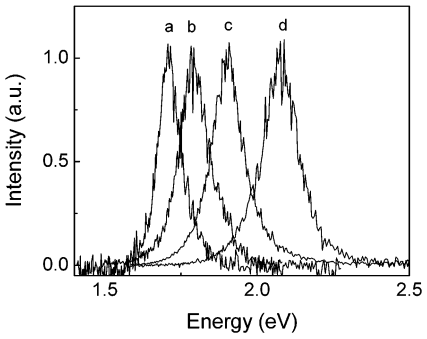


**Figure 6.** Light scattering spectra from single nanoparticles: (a) pure gold nanorods, (b)−(d) core/shell nanorods with increasing thickness of silver shell. The intensities were normalized.

If the particle is inhomogeneous with interfaces, such as the Au/Ag nanorods, dissipation can be accounted separately for each material $i$, and at each interfaces $ij$ such that

$$\gamma_i = \gamma_{0,i} + \sum_j \gamma_{s,ij} = \gamma_{0,i} + \frac{\upsilon_{F,i}}{4V_i}\sum_j A_{ij}S_{ij} \tag{10}$$

where $S_{ij}$ is the interface between material $i$ and material $j$. The plasmon damping constant is then the weighted average of the damping constants of each part,

$$\gamma = \sum_i \beta_i\gamma_i = \sum_i \beta_i\gamma_{0,i} + \sum_i\sum_j \frac{\beta_i\upsilon_{F,i}A_{ij}S_{ij}}{4V_i} = \gamma_0 + \sum_i\sum_j \frac{\beta_i\upsilon_{F,i}A_{ij}S_{ij}}{4V_i} \tag{11}$$

where the weighting factor $\beta_i$ represents the fractions of the total polarization energy in material $i$. $\gamma_0$ is the overall effective volume damping constant. Although the model is phenomenological and based on a classical description that is without a firm basis, we believe that the resulting scaling behavior of the damping rate in terms of surface-to-volume ratios normalized by the polarization energy in each metal component will withstand more accurate treatments.

As shown in Figure 6, single nanocrystal light scattering spectra from gold nanorods, either uncoated or coated with different thicknesses of silver, have a quasi-Lorentzian lineshape. The spectrum (a) is the plasmon resonance of the longitudinal mode of gold nanorods at 1.7 eV, corresponding to aspect ratio 3.0. The line widths were measured to be from 70 to 90 meV, which is similar to the values (∼85 meV) reported by Sönichsen et al.[22] For core/shell nanorods, the plasmon resonance was at 1.75−2.10 eV, the tuning being mostly due to different thicknesses of the silver shell, and a smaller variance in the shape of the gold core. Their line widths were measured to be 100−130 meV, significantly broader than those of pure gold nanorods. In Figure 7, the measured line widths Γ are plotted versus the corresponding peak positions $E_{\text{res}}$ for each sample. Neglecting interfacial scattering, the simulated widths from the model built previously are shown in the dotted line. The dielectric functions are the bulk values. The medium dielectric constant is approximately 2.25 for PVP and immersion oil. For pure gold nanorods, the experimental spectra are less than 10% broader than the theoretical value.

We can model the excess width using eq 8 and a parameter $A_{\text{gm}}$ describing the inelastic scattering at the Au/medium interface. Assuming the nanorod to be a spheroid, its volume

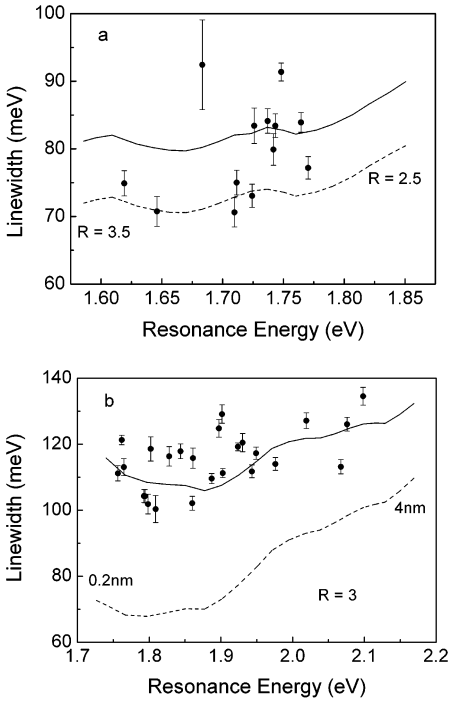


**Figure 7.** (a) Measured line widths Γ of light-scattering spectra of single Au nanorod (dots) vs resonance energy. The dashed line represents the simulated line width for pure Au nanorods with diameter $d = 15$ nm and $R = 3.5 \rightarrow 2.5$, using bulk dielectric function. The solid line accounts for the extra interfacial damping. (b) Measured line widths Γ of light-scattering spectra of a core/shell nanorod (dots) vs the resonance energy. The dashed line is the simulated line width for core/shell nanorods with $d = 15$ nm, $R = 3.0$ Au core and a $0.2 \rightarrow 4.0$ nm Ag shell, using bulk dielectric functions. The solid line accounts for the extra interfacial damping.

is $(4\pi/3)a^3R$, and its surface area is $4\pi a^2R$, where $a$ and $R$ are its short semiaxis and aspect ratio, respectively. Taking $a = 7.5$ nm, $v_{F,Au} = 1.39\ 10^8$cm/s,[32] $\Delta\Gamma$ is added to the $\Gamma - E_{res}$ relation calculated from the bulk dielectric function. To account for the less than 10% excess width, the scattering parameter $A_{gm}$ is found to be 0.1 or less (solid line in Figure 6a). This low value of $A_{gm}$ indicates that the electron−surface scattering is nearly elastic, which confirms the result of Hartland et al.[33]

The core/shell nanorods have two interfaces: one is the Ag/medium interface and the other is the Au/Ag interface. The damping contribution from each interface can be evaluated from eq 10. The gold core is modeled as before. The silver shell is modeled as a homogeneous layer with the thickness used in the spectra simulation, we use $v_{F,Ag} = 1.39 \times 10^8$cm/s.[32] The damping constant of the whole particle is given by eq 11. In the dipole approximation, both the core and the shell are homogeneously polarized, with $\epsilon_{Ag}E_{Ag} = \epsilon_{Au}E_{Au}$. The energy density in a dielectric is $\epsilon E^2/2$; therefore, the fraction of total polarization energy in the Ag shell is $\beta_{Ag} = 1/[1+(\epsilon_{Ag}V_{Au}/\epsilon_{Au}V_{Ag})]$. Correspondingly, $\beta_{Au} = 1 - \beta_{Ag} = 1/[1+(\epsilon_{Au}V_{Ag}/\epsilon_{Ag}V_{Au})]$. The scattering parameter $A_{sm}$ at the Ag−medium interface is assumed to be equal to $A_{gm}$, 0.1, because of the similarity of the electronic structure and lattice structure between Au and Ag. The scattering parameter $A_{gs}$ at the Au/Ag interface is then found to be 0.25 to give a best fit to the experimental values (solid line in Figure 7b). If $A_{sm}$ is zero, and $A_{gs}$ is 0.31, the fit is very similar. Therefore the scattering of conduction electrons at the Au/Ag interface is more inelastic than at the nanorods surface, but not totally inelastic. The slight mismatch between the lattices of Au and Ag may bring a certain amount of defects to the interface, and could be responsible for some of the inelasticity. An alternative explanation to the broader width of the Au/Ag core/shell systems could be scattering at grain boundaries of the thin Ag shell or the rougher outer surface, although within the resolution of the TEM images, the surfaces look of high quality. Such possible additional scattering implies therefore that the value for $A_{gs}$ of ∼0.3 is an upper limit. In contrast to this result, Schatz et al. had previously assumed that the scattering of conduction electrons at an Au/Ag interface is totally inelastic.[26]

It will be of interest to determine if the measured value of the interfacial scattering factor of ∼0.3 between Au and Ag depends on the plasmon energy and on the shape of the interface. The extra damping of a conduction electron at the Au/Ag interface is a disadvantage and it challenges the original idea of taking Au/Ag core/shell nanorods as a replacement for Ag nanorods. Indeed, Ag nanorods at similar energy should have a width of only ∼50meV. However, as shown by Chiang et al., it may be possible that the interfacial inelastic scattering vanishes at sufficiently low energy.[34] Nevertheless, we observed that the width in Au/Ag core/shell nanorods is still less than for pure Au nanorods for $E_{res} > 2$ eV, where the damping from the interband transition of Au becomes dominant.

## 4. Conclusion

Au/Ag core/shell nanorods were synthesized by chemically reducing Ag(I) onto the surface of Au nanorods. The longitudinal plasmon resonance of core/shell nanorods was blue-shifted, as the Ag layer became thicker. We applied a new model based on confocal ellipsoids, with qualitative agreement to the experimental spectra. To evaluate the extra plasmon damping due to the core−shell interface, a dark-field microscope technique was used to measure the light-scattering spectra from single nanocrystals. The line width of core/shell nanorods is about 40−50% broader than the simulation that used bulk dielectric constants, while that of Au nanorods is less than ∼10% broader. A new energy-loss model was presented to evaluate the extra damping of a conduction electron in an arbitrary-shape metal particle. This model leads to a simple result for the damping factor, as $\gamma = \gamma_0 + A(v_F S/4V)$, for a single system. For the core/shell system, a set of electron−surface scattering parameters was chosen for each interface to fit the simulated spectra to the experimental ones. The data can be interpreted to indicate that the scattering is nearly elastic at the metal−medium interface ($A \sim 0.1$), and more inelastic at the Au−Ag interface ($A \sim 0.25$). In the context of using metallic nanoparticles for shaping and enhancing local fields, the added flexibility of making a composite system must be balanced by the added damping due to the interfaces. Further studies of the interfacial scattering might show energy windows where interfacial scattering can be eliminated.

**Acknowledgment.** We acknowledge helpful discussions with Dr. Matthew A. Pelton. This work was supported by the University of Chicago MRSEC under NSF Grant DMR-0213765.

## References and Notes

(1) Fleischmann, M.; Hendra, P. J.; McQuillan, A. J. *Chem. Phys. Lett.* **1974**, *26*, 163.

(2) Jeanmaire, D. L.; Van Duyne, R. P. *J. Electroanal. Chem.* **1977**, *84*, 1.

(3) Kreibig, U.; Vollmer, M. *Optical Properties of Metal Clusters*; Springer-Verlag: Berlin, 1995.

(4) Bohren, C. F.; Huffman, D. R. *Absorption and Scattering of Light by Small Particles*; Wiley: New York, 1983.

(5) Jin, R. C.; Cao, Y. W.; Mirkin, C. A.; Kelly, K. L.; Schatz, G. C.; Zheng, J. G. *Science* **2001**, *294*, 1901.

(6) Link, S.; El-Sayed, M. A. *J. Phys. Chem. B* **1999**, *103*, 8410.
(7) Gans, R. *Ann. Phys.* **1915**, *47*, 270.
(8) Wang, D.-S.; Kerker, M. *Phys. Rev. B* **1981**, *24*, 1777.
(9) Nikoobakht, B.; Wang, J.; El-Sayed, M. A. *Chem. Phys. Lett.* **2002**, *366*, 17.
(10) van der Zande, B. M. I.; Bohmer, M. R.; Fokkink, L. G. J.; Schönenberger, C. *Langmuir* **2000**, *16*, 451.
(11) Yu, Y.-Y.; Chang, S.-S.; Lee, C.-L.; Wang, C. R. C. *J. Phys. Chem. B* **1997**, *101*, 6661.
(12) Jana, N. R.; Gearheart, L.; Murphy, C. J. *J. Phys. Chem. B* **2001**, *105*, 4065.
(13) Kim, F.; Song, J. H.; Yang, P. D. *J. Am. Chem. Soc.* **2002**, *124*, 14316.
(14) Nikoobakht, B.; El-Sayed, M. A. *Chem. Mater.* **2003**, *15*, 1957.
(15) Tornblorn, M.; Henriksson, U. *J. Phys. Chem. B* **1997**, *101*, 6028.
(16) Liu, M. Z.; Guyot-Sionnest, P. Unpublished.
(17) Haynes, C. L.; Van Duyne, R. P. *J. Phys. Chem. B* **2003**, *107*, 7426.
(18) Hodak, J. H.; Martini, I.; Hartland, G. V. *J. Phys. Chem. B* **1998**, *102*, 6958.
(19) Ah, C. S.; Hong, S. D.; Jang, D.-J. *J. Phys. Chem. B* **2001**, *105*, 7871.
(20) Klar, T.; Perner, M.; Grosse, S.; von Plessen, G.; Spirkl, W.; Feldmann, J. *Phys. Rev. Lett.* **1998**, *80*, 4249.
(21) Sönnichsen, C.; Geier, S.; Hecker, N. E.; von Plessen, G.; Feldmann, J.; Ditlbacher, H.; Lamprecht, B.; Krenn, J. R.; Aussenegg, F. R.; Chan, V. Z-H.; Spatz, J. P.; Möller, M. *Appl. Phys. Lett.* **2000**, *77*, 2949.
(22) Sönnichsen, C.; Franzl, T.; Wilk, T.; von Plessen, G.; Feldmann, J.; Wilson, O.; Mulvaney, P. *Phys. Rev. Lett.* **2002**, *88*, 077402.
(23) Raschke, G.; Kowarik, S.; Franzl, T.; Sönnichsen, C.; Klar, T. A.; Feldmann, J.; Nichtl, A.; Kurzinger, K. Nano Lett. **2003**, *3*, 935.
(24) McFarland, A. D.; Van Duyne, R. P. *Nano Lett.* **2003**, *3*, 1057.
(25) Mock, J. J.; Barbic, M.; Smith, D. R.; Schultz, D. A.; Schultz, S. *J. Chem. Phys.* **2002**, *116*, 6755.
(26) Kim, Y.; Johnson, R. C.; Li, J.; Hupp, J. T.; Schatz, G. C. *Chem. Phys. Lett.* **2002**, *352*, 421.
(27) Dielectric functions of Ag and Au for the simulation are from Johnson, P. B.; Christy, R. W. *Phys. Rev. B* **1972**, *6*, 4370. $\epsilon_m = 1.77$ refers to water at room temperature.
(28) Arbouet, A.; Voisin, C.; Christofilos, D.; Langot, P.; Del Fatti, N.; Vallée F.; Lermé, J.; Celep, G.; Cottancin, E.; Gaudry, M.; Pellarin, M.; Broyer, M.; Maillard, M.; Pileni, M. P.; Treguer, M. *Phys. Rev. Lett.* **2003**, *90*, 177401.
(29) Coronado, E. A.; Schatz, G. C. *J. Chem. Phys.* **2003**, *119*, 3926.
(30) Kreibig, U.; Fragstein, C. V. *Z. Phys.* **1969**, *224*, 307.
(31) Kreibig, U. *Z. Phys.* **1970**, *234*, 307.
(32) Kittel, C. *Introduction to solid-state physics*, 6th ed.; Wiley: New York, 1986.
(33) Hodak, J. H.; Martini, I.; Hartland, G. V. *J. Phys. Chem. B* **1998**, *102*, 6958.
(34) McMahon, W. E.; Miller, T.; Chiang, T.-C. *Phys. Rev. Lett.* **1993**, *71*, 907.